"Includes online access to fully searchable text and images!"

MRI of the Musculoskeletal System

Sixth Edition

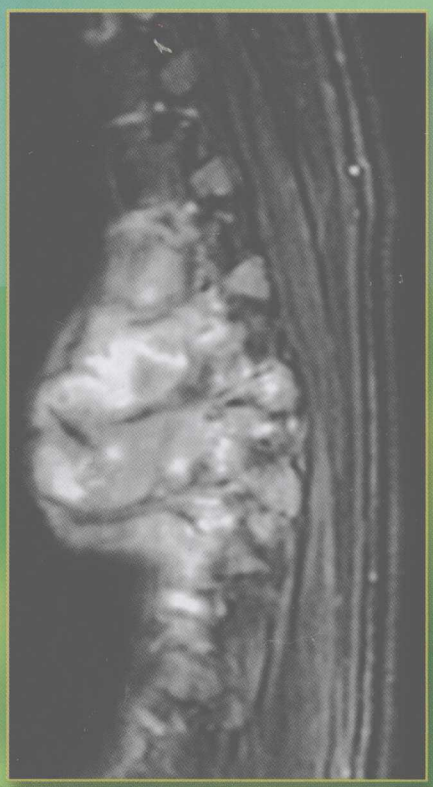

Thomas H. Berquist

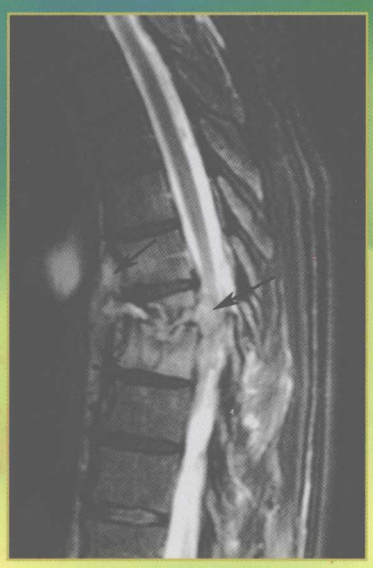

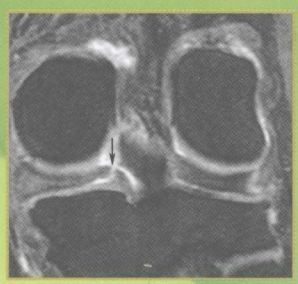

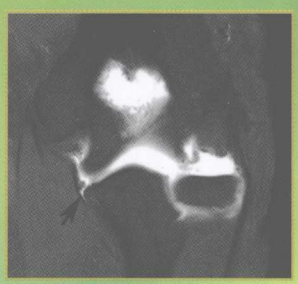

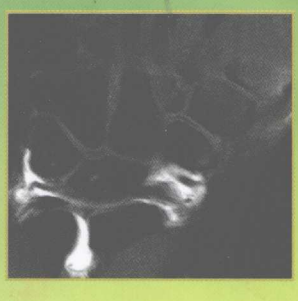

Wolters Kluwer Health | Lippincott Williams & Wilkins

MRI of the Musculoskeletal System

SIXTH EDITION

EDITOR

Thomas H. Berquist, MD, FACR

Consultant, Department of Diagnostic Radiology
Mayo Clinic
Jacksonville, Florida

Professor of Diagnostic Radiology
Mayo Medical School
College of Medicine
Mayo Foundation
Rochester, Minnesota

Wolters Kluwer Health | Lippincott Williams & Wilkins

Philadelphia • Baltimore • New York • London
Buenos Aires • Hong Kong • Sydney • Tokyo

Senior Executive Editor: Jonathan Pine
Product Manager: Ryan Shaw
Vendor Manager: Alicia Jackson
Senior Manufacturing Manager: Benjamin Rivera
Senior Marketing Manager: Caroline Foote
Design Coordinator: Holly McLaughlin
Production Service: Aptara, Inc.

Two Commerce Square
2001 Market Street
Philadelphia, PA 19103 USA
LWW.com

Printed in China

Library of Congress Cataloging-in-Publication Data

MRI of the musculoskeletal system / editor, Thomas H. Berquist. – 6th ed.
p. ; cm.
Includes bibliographical references and index.
Summary: "MRI of the Musculoskeletal System is a classic one-volume textbook on all aspects of MR msk imaging. It covers basic principles of interpretation, physics, and terminology before moving through a systematic presentation of disease region of the body. The new edition will include new pulse sequences and artifacts in the basics chapters; enhanced anatomy artwork; and new images and figures on greater trochanteric pain syndrome and other new disorders in the hips and thighs. It will also include more arthrography in the hand and shoulder chapters, and more emphasis on shoulder acroniums and injury patterns. The infection chapter will add new infection categories and will increase emphasis on the diabetic foot"–Provided by publisher.
ISBN 978-1-4511-0918-4 (hardback : alk. paper)
I. Berquist, Thomas H. (Thomas Henry), 1945-
[DNLM: 1. Musculoskeletal Diseases–diagnosis. 2. Magnetic Resonance Imaging–methods. 3. Musculoskeletal System–anatomy & histology. WE 141]
616.7′07548–dc23 2011050213

To purchase additional copies of this book, call our customer service department at (800) 638-3030 or fax orders to (301) 223-2320. International customers should call (301) 223-2300.

Visit Lippincott Williams & Wilkins on the Internet: at LWW.com. Lippincott Williams & Wilkins customer service representatives are available from 8:30 am to 6 pm, EST.

10 9 8 7 6 5 4 3 2 1

RRS1203

MRI of the Musculoskeletal System

SIXTH EDITION

To my loving wife, Mary, for her continued support of my writing throughout the years.

Preface

The fifth edition of *MRI of the Musculoskeletal* System was published in 2006. Since the last edition, magnet configurations have become more diverse and the use of 3.0 Tesla and higher field systems have become more common for clinical imaging. New multichannel phased array coils and pulse sequences have also been developed to improve imaging capabilities for musculoskeletal imaging. Gadolinium is more commonly used for conventional imaging, direct MR arthrography, and angiography. The need to address potential complications of this contrast agent, specifically nephrogenic system sclerosis, has also changed the use of this agent in specific clinical settings. Spectroscopy continues to lag behind as a commonly used tool for clinical studies.

The sixth edition of *MRI of the Musculoskeletal System* provides significant updates related to imaging approaches and the expanded applications of MRI for musculoskeletal disorders. There are approximately 50% new images and references in this edition. Chapter 1 continues to update basic physics principles, pulse sequences, and terminology providing an easy to read, clinically useful approach to these basic principles. Chapter 2 provides essentials of interpretation regarding tissue contrast, lesion conspicuity, and necessary approaches for appropriate image interpretation. Chapter 3 provides basic technology principles to avoid redundancy in subsequent chapters. Discussions include patient selection, safety issues, patient positioning, coil selection, pulse sequences, and the use of gadolinium for conventional, arthrographic, and angiographic imaging. Contrast reactions and concerns regarding the use of gadolinium agents are also addressed. Chapter 3 also discusses sedation issues in adults and children.

Chapters 4 to 11 are anatomically oriented as in the past editions of this text. There are numerous new anatomic illustrations and expanded technical discussions related to the specific anatomic regions in these chapters. New applications are included in each chapter as well as pediatric conditions, where appropriate. Chapter 5 is significantly different compared with the last edition in that there is more emphasis on spondyloarthropathies and other spinal and perispinal musculoskeletal conditions. The non-degenerative neuroradiology emphasis has been reduced.

Chapter 12 provides a thorough discussion of staging and imaging of musculoskeletal neoplasms and tumorlike conditions. There are thorough discussions regarding tumor staging, imaging approaches to benign and malignant bone and soft tissue lesions, and biopsy approaches. Chapter 13 provides an in-depth discussion of osseous, articular, and soft tissue infections. Chapter 14 covers diffuse marrow disorders. This chapter has also been updated significantly compared with the fifth edition. Chapter 15 discusses miscellaneous and evolving MR applications. The final chapter, Chapter 16, updates the clinical utility of MR spectroscopy.

The new and evolving techniques and applications for musculoskeletal MRI are addressed in this new edition. New anatomic, technical, and clinical applications are reviewed. The updated sixth edition of MRI of the Musculoskeletal System will be useful to students, residents in training, and all physicians responsible for requesting and interpreting musculoskeletal MR examinations. Appropriate selection of MRI studies and optimization of their use is increasingly important in the era of health care reform.

Acknowledgments

Preparation of this text could not have been accomplished without the support of my fellow faculty, fellows, and residents who assisted with case selection and technical suggestions. I especially want to acknowledge Lisa Broddle and Tony Schroeder for their assistance with cases selection, photos demonstrating patient positioning, and coil techniques.

My secretary, Kathryn Hatcher, was instrumental in obtaining permissions and keeping me on task with production issues. As always, a special thanks to John Hagen for the artwork provided in the new edition and all previous editions of this text.

Finally, I would like to thank Ryan Shaw and the staff at Wolters Kluwer/Lippincott Williams & Wilkins for assistance in the development and editing of this text.

Contributors

Laura W. Bancroft, MD
Clinical Professor of Radiology
Florida State University School of Medicine
Tallahassee, Florida
Adjunct Professor of Radiology
University of Central Florida School of Medicine
Orlando, Florida

Thomas H. Berquist, MD
Consultant
Department in Diagnostic Radiology
Mayo Clinic, Jacksonville, Florida
Professor of Diagnostic Radiology
Mayo Medical School
College of Medicine
Rochester, Minnesota

Daniel F. Broderick, MD
Consultant in Diagnostic Radiology
Mayo Clinic
Jacksonville, Florida
Assistant Professor of Diagnostic Radiology
Mayo Medical School
College of Medicine
Rochester, Minnesota

Mark S. Collins, MD
Consultant
Department of Diagnostic Radiology
Rochester, Minnesota
Assistant Professor of Diagnostic Radiology
Mayo Medical School
College of Medicine
Rochester, Minnesota

Richard L. Ehman, MD
Consultant
Department of Diagnostic Radiology
Rochester, Minnesota
Professor of Diagnostic Radiology
Mayo Medical School
College of Medicine
Rochester, Minnesota

Joel P. Felmlee, PhD
Consultant
Department of Diagnostic Radiology
Rochester, Minnesota
Professor of Diagnostic Radiology
Mayo Medical School
College of Medicine
Rochester, Minnesota

Mark J. Kransdorf, MD
Consultant
Department of Diagnostic Radiology
Mayo Clinic
Jacksonville, Florida
Professor of Diagnostic Radiology
Mayo Medical School
College of Medicine
Rochester, Minnesota

Richard L. Morin, PhD
Consultant in Radiologic Physics
Mayo Clinic
Jacksonville, Florida
Brooks-Hollern Professor
Professor of Radiologic Physics
Mayo Medical School
College of Medicine
Rochester, Minnesota

William A. Murphy, Jr., MD
Professor of Radiology
Department of Diagnostic Radiology
University of Texas
MD Anderson Cancer Center
Houston, Texas

Jeffrey J. Peterson, MD
Consultant
Department of Diagnostic Radiology
Mayo Clinic
Jacksonville, Florida
Professor of Diagnostic Radiology
Mayo Medical School
College of Medicine
Rochester, Minnesota

Robert A. Pooley, PhD
Consultant in Radiologic Physics
Department of Diagnostic Radiology
Mayo Clinic
Jacksonville, Florida
Assistant Professor of Radiologic Physics
Mayo Medical School
College of Medicine
Rochester, Minnesota

James B. Vogler III, MD
Clinical Associate Professor of Radiology
Department of Radiology
University of Florida College of Medicine
Gainesville, Florida
Co-director Invision Outpatient Imaging Center
North Florida Regional Medical Center
Gainesville, Florida

Contents

1 Basic Principles and Terminology of Magnetic Resonance Imaging

Robert A. Pooley • Joel P. Felmlee • Richard L. Morin

This chapter is presented to acquaint those new to magnetic resonance imaging (MRI) with the fundamental concepts and basic principles responsible for the nuclear magnetic resonance (NMR) phenomenon and MRI. At the outset, it is important to understand that this chapter is intended to be tutorial in nature. In addition to the fundamental concepts of the physical phenomenon of NMR itself, techniques relevant to clinical imaging are discussed in the context of a tutorial presentation of fundamentals for those new to MRI. It is important to appreciate that the physics principles associated with MRI often take a while to assimilate. There are many approaches to the discussion and presentation of the fundamental physics of MRI. Technical details and in-depth coverage can be found in MRI texts and review articles.[1–5] The appendix lists terms that have been selected from the American College of Radiology glossary of MR terms[6] and are provided for the sake of completeness and reference.

A chronology of the historical development of MRI is listed in Table 1.1. The principle of NMR was first elucidated in the late 1940s by Professor Bloch at Stanford and Professor Purcell at Harvard. In 1952, they shared the Nobel Prize in physics for their work. The importance of this technique lies in the ability to define and study the molecular structure of the sample under investigation. In the 1970s, the principle of NMR was utilized to generate cross-sectional images similar in format to X-ray computed tomography (CT). By 1981, clinical research was underway.

The intense enthusiasm and the rapid introduction of MRI into the clinical environment stem from the abundance of diagnostic information present in MR images. Although the image format is similar to that of CT, the fundamental principles are quite different; in fact, an entirely different part of the atom is responsible for the image formation. In MRI it is the *nucleus* that provides the signal used in generating an image. We note that this differs from conventional diagnostic radiology in which the *electrons* are responsible for the imaging signal. Furthermore, it is not only the nucleus of the atom but also its structural and biochemical environments that influence the signal.

Currently, fast imaging techniques are increasing as important clinical methods. Echo planar imaging (EPI), as well as fast spin echo and gradient echo based acquisitions, allows image acquisition in the sub-second to breath hold (15 second) range. These techniques hold the potential for high-resolution studies acquired quickly, thereby "freezing" many physiologic motions. Using these fast acquisition techniques, encoding functional and flow information into the image are areas of clinical interest and research.

Throughout this discussion we illustrate the underlying physics principles with analogies and discuss the nature of the physics from a "classical" rather than a "quantum mechanical" point of view. Both approaches result in accurate explanations of the NMR phenomenon; however, they differ in their mathematical constructs and visualization of the underlying physical principles.

THE NUCLEAR MAGNETIC RESONANCE EXPERIMENT

When certain nuclei (those with an odd number of protons, an odd number of neutrons, or an odd number of both) are placed in a strong magnetic field, they align themselves with the magnetic field and begin to rotate at a precise rate or frequency (Larmor frequency). If a radio transmission is made at this precise frequency, the nuclei will absorb the radio frequency (RF) energy and become "excited." After termination of the radio transmission, the nuclei will calm down

Table 1.1 Historical Development of MRI

1946	Elucidation of NMR phenomena and technique – Bloch, Purcell
1951	Single dimension spatial localization – Gabillard
1952	Nobel Prize to Bloch and Purcell
1959	Blood flow by NMR – Singer
1971	In Vitro cancer detection by NMR – Damadian
1972	In Vivo cancer detection by NMR – Weisman
1972	NMR Imaging – Damadian
1973	NMR Zeugmatography – Lauterbur
1975	Commercial development
1981	Clinical trials with prototypes

(or relax) with the emission of radio waves. The emission of RF energy as the nuclei relax is the source of the NMR signal. The ability of a system to absorb energy that is "packaged" in a particular kind of way is termed *resonance*. This condition is analogous to the pushing of a child on a swing. If the child is pushed at the highest point of return, then the maximum amount of energy is transmitted to the swing. Attempting to push the child at the midpoint of return results in a low transfer of energy, and in this sense would be *off-resonance*. Hence, the resonance condition in this case is the timing of pushes with the exact frequency of the pendulum movement of the swing.

The precession of nuclei about a magnetic field is similar in concept to the precession of a spinning top in the presence of a gravitational field, as illustrated in Figure 1.1. This type of rotation occurs whenever a spinning motion interacts with another force. Nuclei with an odd number of protons or neutrons or both possess a property of "spin," which in this case interacts with the magnetic field, thereby inducing precession of the nuclei about the magnetic field. The precessional or Larmor frequency is determined by the individual nuclei and the magnetic field strength [given in the SI unit Tesla (T) or the centimeter–gram–second (cgs) unit gauss (G), where 1T = 10,000 G]. The mathematical definition of the Larmor frequency is given by

$$\omega = \gamma B_0,$$

where ω is the Larmor frequency, B_0 is the static magnetic field strength, and γ is the gyromagnetic ratio (a constant that is different for each nucleus). Larmor frequencies for various nuclei and field strengths are given in Tables 1.2 and 1.3. For protons at a field strength of 1.5T, the Larmor frequency is 64 megahertz (MHz), which is the same frequency used for transmitting the television signal of channel 3.

In summary, the fundamentals of the NMR experiment are illustrated in Figure 1.2 and consist of three steps: (a) placing a sample in a magnetic field, thereby inducing a nuclear precession, (b) transmitting an RF pulse at the Larmor frequency, and (c) "listening" for the returning NMR signal. Note that the frequency of the transmitted RF and the returning signal are dependent upon both the nuclei of interest and the magnetic field strength B_0.

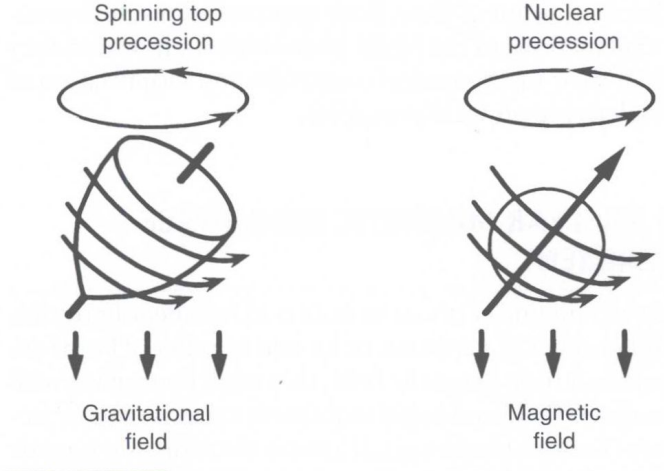

Figure 1.1 Illustration of precession. (Adapted from Fullerton GD. Basic concepts for nuclear magnetic resonance imaging. *Magn Reson Imaging*. 1982;1:39–55, with permission.)

Table 1.2 Larmor (Resonance) Frequencies for Hydrogen

Field Strength (Tesla)	Resonance Frequency (MHz)
0.15	6.4
0.35	14.9
0.50	21.3
1.00	42.6
1.50	63.9
2.00	85.2
4.00	170.3

THE NUCLEAR MAGNETIC RESONANCE SIGNAL

The form of the RF signal produced by the NMR experiment depends on the number of nuclei present (spin density) and the time it takes for the nuclei to relax (T1 and T2). The parameter T1 (spin–lattice relaxation time) measures the rate of return of the nuclei to alignment with the static magnetic field (B_0) and reflects the chemical environment of the proton. T2 (spin–spin relaxation time) measures the dephasing of the nuclei in the transverse plane and reflects the relationship of the proton to the surrounding nuclei.

Table 1.3 Larmor (Resonance) Frequencies AT 1.0 Tesla

Nucleus	Larmor Frequency (MHz)
1H	42.6
13C	11.0
14N	3.0
31P	17.1

H, hydrogen; C, carbon; N, nitrogen; P, phosphorus.

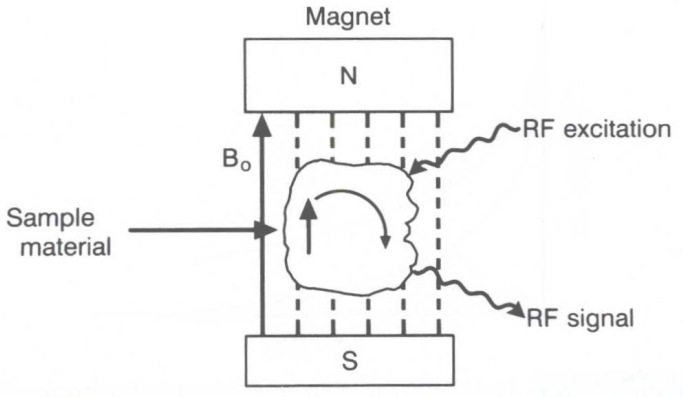

Figure 1.2 Basics of NMR measurements. Here the magnetization is nutated 90° by the RF excitation. (Adapted from Fullerton GD. Basic concepts for nuclear magnetic resonance imaging. *Magn Reson Imaging*. 1982;1:39–55, with permission.)

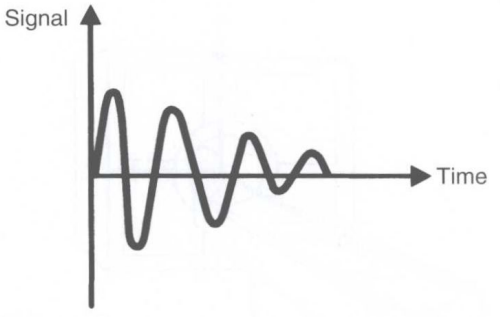

Figure 1.4 Plot of free induction decay (FID), the basic NMR signal.

These processes are illustrated in Figure 1.3. The degree to which the NMR signal depends on spin density, T1 or T2, is determined by the pulse sequence, which we shall discuss later. The nature of this signal and its decay due to relaxation are of fundamental importance and we shall discuss this process in detail.

The form of the basic NMR signal [free induction decay (FID)] is shown in Figure 1.4. The signal is a time oscillating waveform that is detected in the x-y or transverse plane, defined by the coordinate system for the experiment as shown in Figure 1.5. Note that after a 90° rotation, the magnetization vector is in the "transverse" plane. The received signal is oscillating because we measure it from the transverse plane as the magnetization vector rotates about the longitudinal axis. Hence, a rotating signal is translated into a sinusoidal time-varying voltage.

It is important to understand that we can only measure the macroscopic magnetization vector, that is, the algebraic summation of all nuclear spins under investigation (Fig. 1.6). In reality, not all nuclear spins in a sample precess at the same frequency. Each individual nucleus is influenced by a slightly different magnetic field due to the interactions of electrons that surround individual nuclei or the movements of adjacent molecules. The first process that occurs upon RF transmission is the phasing of individual nuclear spins to create the macroscopic magnetization vector $\mathbf{M}_{xy}$ (similar to the military command "fall in" given to a group of soldiers). This ensemble of phased nuclear spins then changes their orientation with regard to the *z*-axis. The rotation of this phased macroscopic magnetic vector is the property that we detect causing an oscillatory MR signal with time.

The decay of the signal as shown in Figure 1.4 occurs because following cessation of the RF transmission, the nuclear spins dephase. Since magnetization is a vector quantity, dephasing causes the macroscopic magnetic vector to decrease in magnitude. Since this activity takes place in the *x-y* or transverse plane, this process is also called *transverse relaxation*. In a chemical sense, this relaxation is due to interactions that occur between adjacent nuclei and is therefore termed *spin–spin relaxation*. The effect of T2

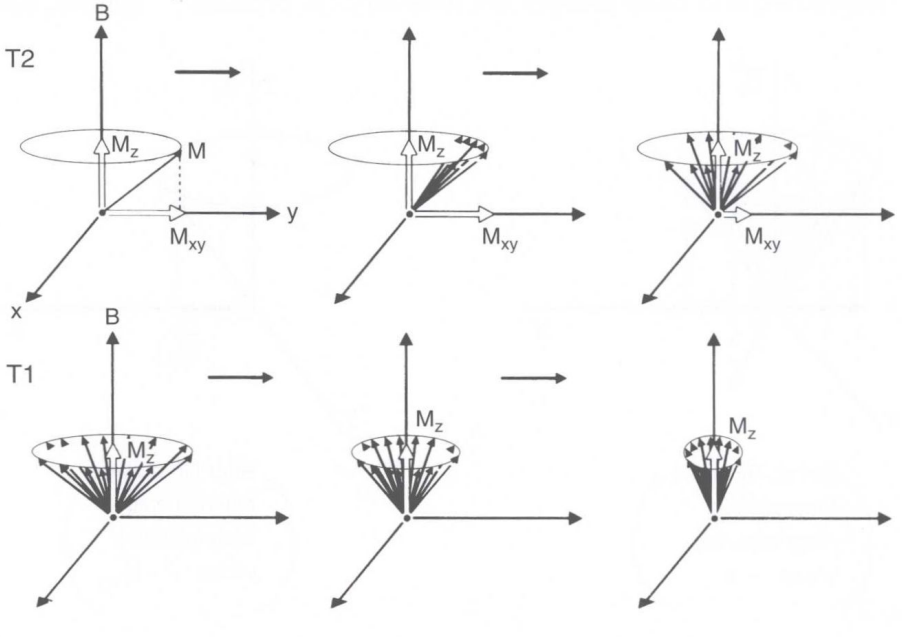

Figure 1.3 Diagram of T2 (spin–spin, transverse) relaxation and T1 (spin-lattice, longitudinal) relaxation after a 90° nutation pulse.

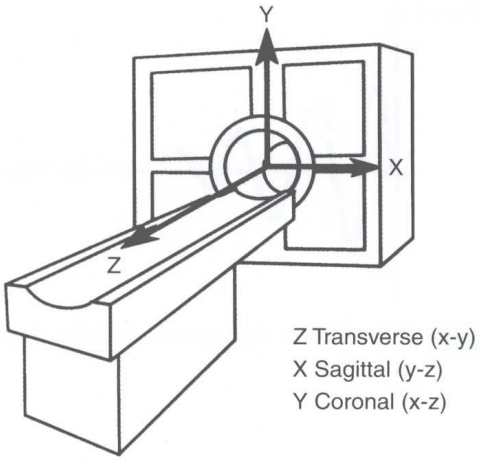

Figure 1.5 MRI coordinate system.

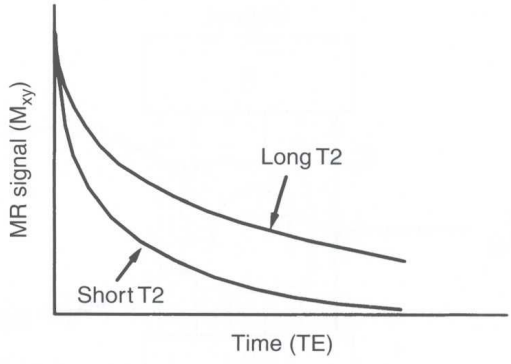

Figure 1.7 Plot of the loss of magnetization in the transverse (xy) plane following cessation of RF transmission.

relaxation for substances with different T2 values is illustrated in Figure 1.7.

As the above-mentioned dephasing or T2 relaxation occurs, the entire ensemble of nuclei return to alignment with the main magnetic field B_0, which is oriented along the *z*-axis. Hence, the longitudinal or *z* component of the macroscopic magnetic vector "grows" or increases with time, as the protons realign with B_0 and return to an equilibrium value. Since this T1 recovery occurs along the direction of the longitudinal axis, it is termed *longitudinal relaxation.* In a chemical sense, this process is governed by the strength with which an individual nucleus is bound to its chemical backbone (water, lipid, protein, etc.) and hence this process is often termed *spin–lattice relaxation.* The effect of T1 relaxation is represented in Figure 1.8 for substances of different T1 values.

MAGNETIC RESONANCE IMAGING

An illustration of an MRI system is shown in Figure 1.9. To conduct the NMR experiment, a strong magnet, radio transmitter, and radio receiver are necessary. To produce MR images, additional magnetic coils (gradient coils) are necessary to encode the signal and thus allow its origin to be determined. In addition, a computer system is necessary to control the sequencing of the RF, gradients, data collection, operations, and perform the final image reconstruction.

In the most common type of MRI, spatial localization is obtained using additional magnetic fields superimposed on the main magnetic field. The key to understanding this phenomenon lies in the Larmor equation. Recall that the precessional frequency is directly related to magnetic field strength. If a spatially varying magnetic field is superimposed on the main magnetic field, then precessional frequencies will be related to a location in space, analogous to the frequency obtained by the specific location of keys on a piano. This translation between frequency and spatial location is shown in Figure 1.10.

The most common imaging technique [two-dimensional Fourier transform or (2DFT)][7–9] involves the use of three such gradient fields to localize a point in space. It is important to understand that all three gradients will be turned on and off at different times. The particular application and relative timing of the *x*, *y*, and *z* gradients determine which axis (*x*, *y*, or *z*) is being localized. In general, signals will be localized by selective application of

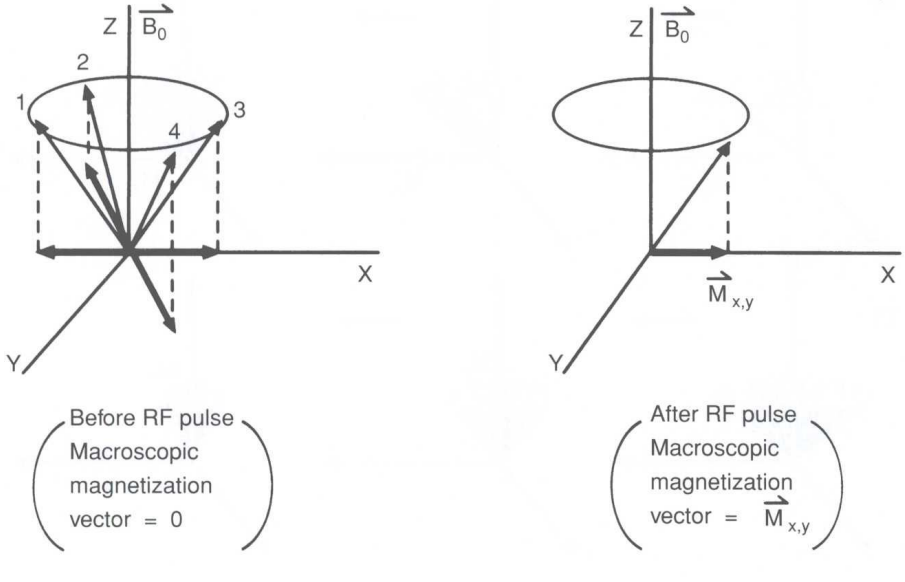

Figure 1.6 Illustration of the macroscopic magnetic vector formed by individual nuclei. **A:** Individual nuclei 1, 2, 3, and 4 precessing about the magnetic field B_0. The measured macroscopic magnetization vector is zero due to the algebraic summation of x and y components of the randomly oriented nuclei. **B:** Macroscopic magnetization vector formed by the phasing of individual nuclei 1, 2, 3, and 4. The macroscopic magnetization vector measured is the component in the transverse plane, that is, $\mathbf{M}_{x,y}$.

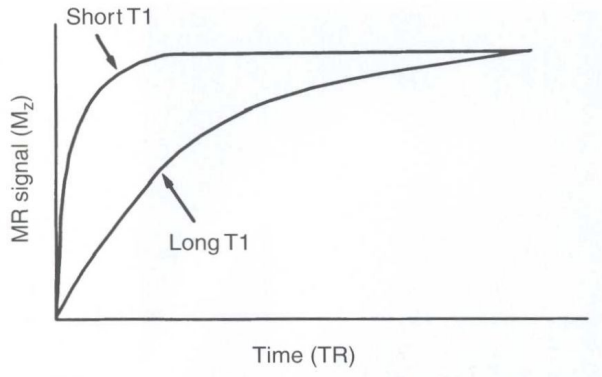

Figure 1.8 Plot of recovery of magnetization in the longitudinal (*z*) direction.

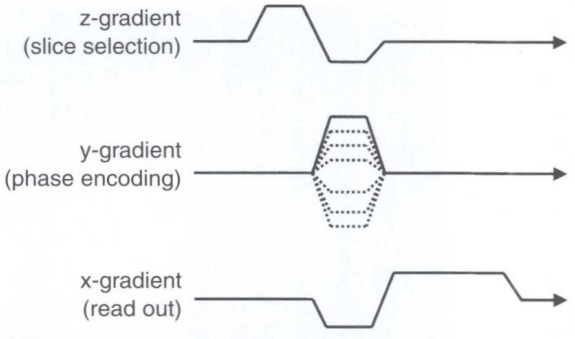

Figure 1.11 Gradient activation versus time for MRI acquisition of a single transverse slice. For this case, slice selection is in the craniocaudal (C–C) direction, phase encoding in the anteroposterior (A–P) direction, and frequency encoding in the right-left (R–L) direction.

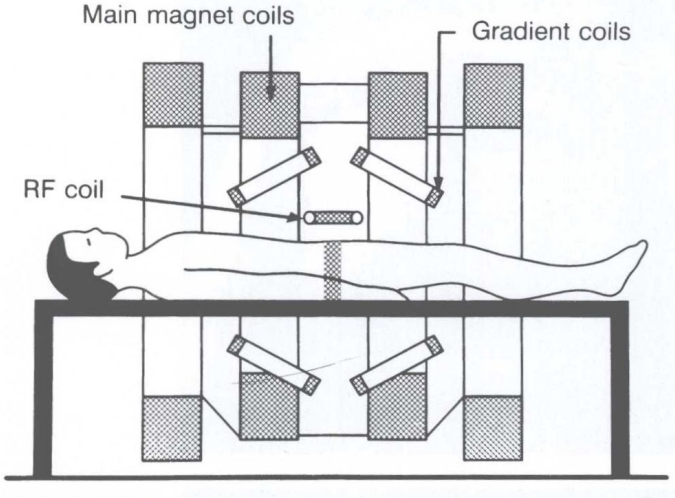

Figure 1.9 Diagram of MRI system. ((Adapted from Fullerton GD. Basic concepts for nuclear magnetic resonance imaging. *Magn Reson Imaging*. 1982;1:39–55, with permission.)

slice selection, phase encoding, and frequency encoding gradients. A schematic diagram of the timing of these gradients is given in Figure 1.11. We describe each in detail for the acquisition of a transverse slice.

The slice is first selected by applying a gradient along the *z*-axis while applying an RF pulse with a narrow frequency range. This excites the nuclei only in the slice of interest so that they are all precessing at the same frequency and phase (Fig. 1.10). However, the signal we detect is from the entire slice, so at this point it is not possible to form an image.

Next, the relative phase of spin precession is modified by applying a gradient in the *y*-direction. This gradient causes the atoms at different location along *y* to precess at different frequencies while the *y* gradient is applied (Fig. 1.12). If no gradient is present, the nuclei precess at the Larmor frequency corresponding to the main magnetic field strength. If a slightly higher magnetic field is superimposed with a gradient as shown in Figure 1.12, the nuclei in row 1 precess at a slightly higher frequency than those in row 2; likewise for rows 2 and 3. When the gradient is turned off, all the rows will once again precess at the same frequency. However, since row 1 was previously precessing at a slightly higher frequency than row 2, all the nuclei in row 1 will be slightly ahead of those in row 2; that is, they will be precessing at the same

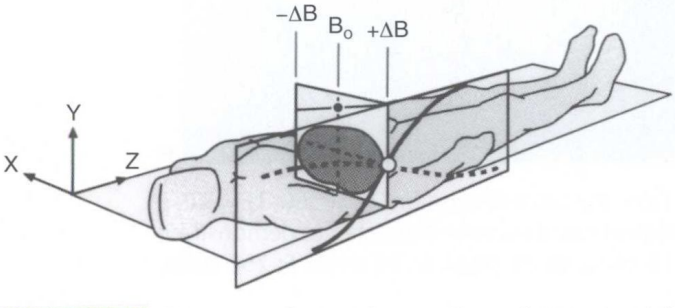

Figure 1.10 Diagram of spatial encoding of MR signal by superposition of magnetic field gradients (different resonance frequencies correspond to different positions along the gradient).

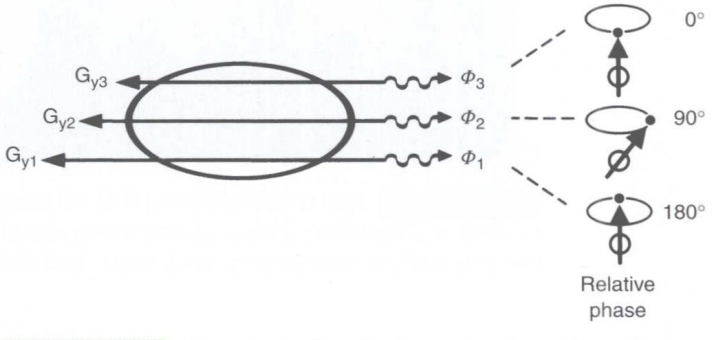

Figure 1.12 Phase encoding in the y-direction. Here the gradient increases from top to bottom.

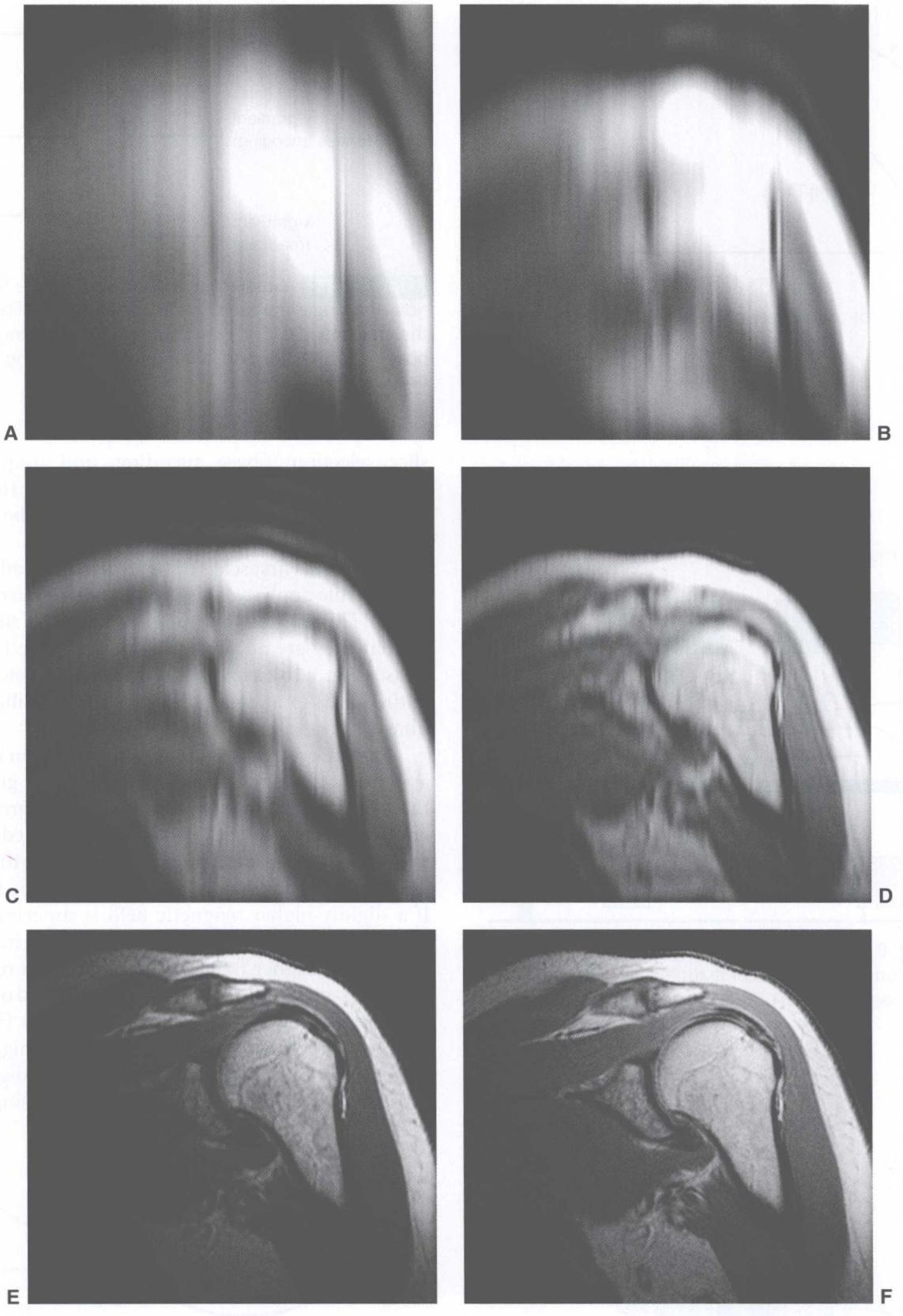

Figure 1.13 MRI phase encoding (10). All images are from the same acquisition (TR = 500, TE = 20, 2 excitation, 5 mm slice, 256 phase encoding steps). The original raw data were truncated to demonstrate the effect of phase encoding. **A:** 2 steps. **B:** 8 steps. **C:** 16 steps. **D:** 32 steps. **E:** 64 steps. **F:** 256 steps.

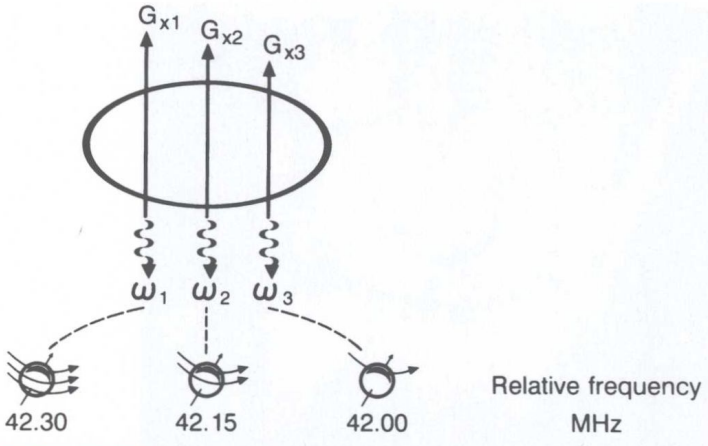

Figure 1.14 Frequency encoding in the x-direction. Here the gradient decreases from left to right.

frequency but at different phases. Likewise, each successive row will precess at the same frequency but at a slightly different phase. To obtain discrimination in the phase encoding direction, this process must be repeated many (e.g., 256) times. This result of increased phase encoding for a coronal image with phase encoding in the superoinferior direction is shown pictorially in Figure 1.13.[10]

The precessing nuclei are frequency encoded by the application of a magnetic gradient in the *x*-direction. This gradient causes the atoms to precess at different frequencies (Fig. 1.14) and is usually applied while the MR signal is being collected (hence, it is sometimes called the readout gradient).

The MR signal is digitized and stored on the acquisition workstation (in "k-space") for subsequent Fourier reconstruction to form the clinical image. Each point in k-space represents a different *spatial frequency* in the object being imaged. The strength of the MR signal (and thus the value of a data point in k-space) indicates the degree to which that spatial frequency is represented in the object. Lower spatial frequencies are located near the center of k-space and contain information related to image contrast. Higher spatial frequencies are located at the periphery of k-space and contain information related to image sharpness. This is demonstrated in Figure 1.15 by viewing k-space and the clinical images reconstructed from the center or periphery of k-space.

MAGNETIC RESONANCE IMAGING PULSE SEQUENCES

MRI pulse sequences are basically the recipe for the application of RF pulses, the sequencing of gradient pulses in the *x*, *y*, and *z* direction, and the acquisition of the resultant MR signal.

The most basic component of a pulse sequence is the specification of the RF excitation and subsequent signal detection. Timing diagrams for two pulse sequences [inversion recovery (IR) and spin echo (SE)] are given in Figures 1.16 and 1.17. Each sequence is discussed in detail.

The schematic diagram for the IR pulse sequence is shown in Figure 1.16. This sequence is characterized by the application of an RF pulse of sufficient power to tip the nuclei through 180°, an inversion time (TI), and the subsequent application of a 90° pulse (to rotate the magnetization into the transverse plane), followed by signal detection. This pulse sequence can be used to measure the longitudinal recovery of magnetization (Fig. 1.18). Because the range of measured magnetization for this pulse sequence varies from $-M_z$ to $+ M_z$, if phase-sensitive image reconstruction is employed, the magnitude of measured differences for a sample due to T1 relaxation may be larger with the IR sequence than those with the spin-echo technique below (in which the longitudinal magnetization varies from 0 to $+M_z$). These differences may not be as pronounced with magnitude reconstruction (Fig. 1.18). Hence, image contrast due to T1 differences can be greater with IR. Examples of images acquired using this pulse sequence and magnitude reconstruction are shown in Figure 1.19.

The pulse diagram for the SE pulse sequence is shown in Figure 1.17. The spin-echo pulse sequence is characterized by the application of a 90° pulse, which therefore tips the nuclei into the transverse or x-y plane. This is followed by successive 180° pulses, separated by the delay period TE, which causes the formation of successive signals for detection, which are termed spin echoes. The entire pulse sequence is repeated following the delay interval TR. The formation of spin echoes is demonstrated in Figure 1.20. The fundamental characteristic of this sequence lies in the fact that the nuclei dephase following the 90° pulse. If this dephasing spin system is rotated through 180°, individual spins will now travel toward one another instead of away from one another. When all spins meet one another, a spin echo is produced. Following that moment in time, the spin system will once again dephase and can be refocused or rephased with another 180° pulse. Depending upon the acquisition TE and TR, this sequence can be useful in demonstrating differences due to either T1 or T2 relaxation time as shown in Figure 1.21. Examples of images acquired using this pulse sequence are given in Figure 1.22. In summary, the spin density, T1, and T2 represent inherent properties of tissues. TE and TR are properties of the image acquisition that are under operator control. The TE and TR of an image acquisition can be manipulated such that the difference between signals from tissues (which ultimately determines the image contrast) is weighted by tissue spin density, T1, or T2 relaxation.

The previous discussion dealt with pulse sequences that were concerned only with RF excitation and signal detection. Hence, this discussion would be germane to spectroscopy as well as imaging. For MRI, the pulse sequence must also identify the timing information associated with the gradients necessary to prepare or localize the signal for image reconstruction.

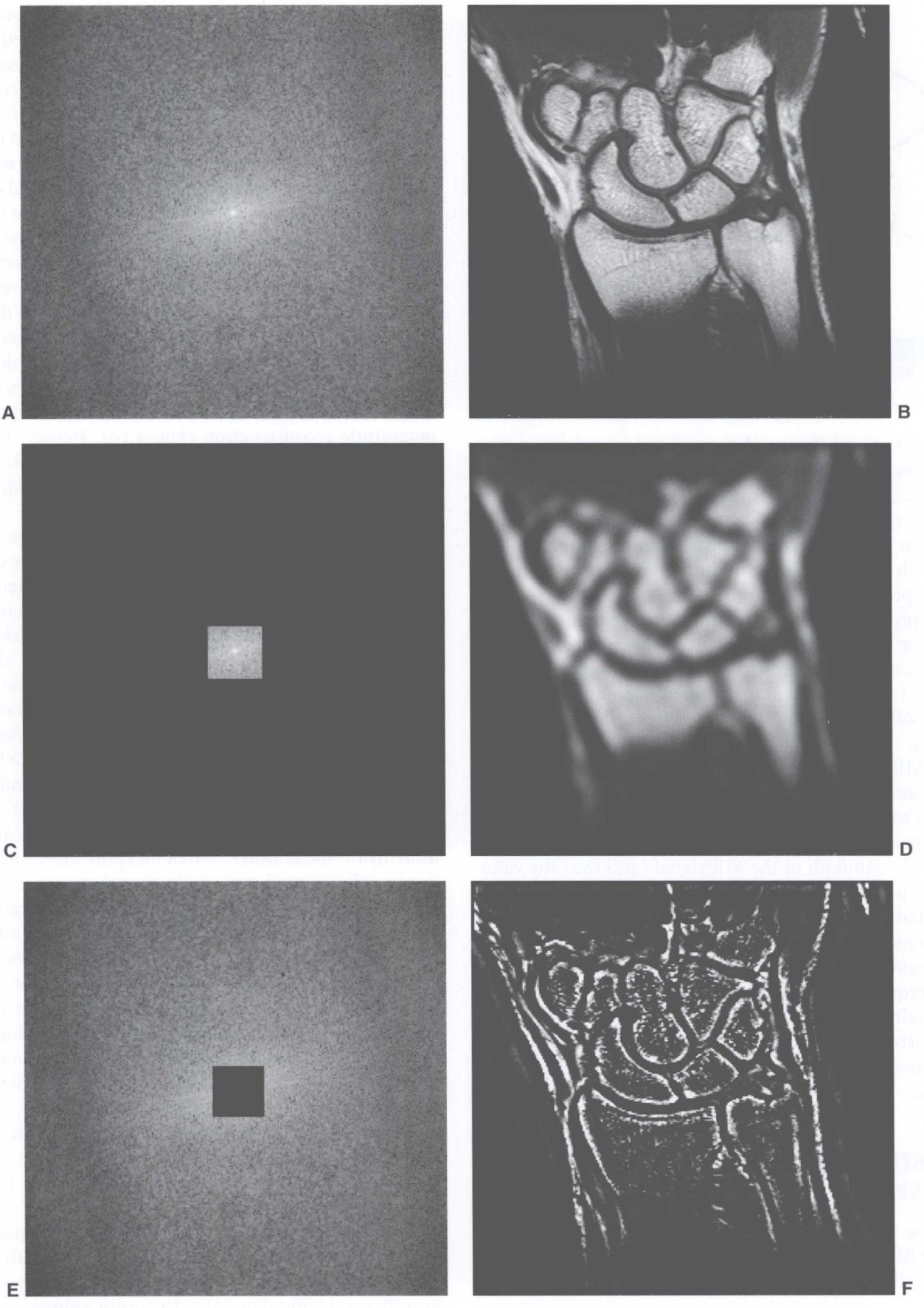

Figure 1.15 Reconstruction of k-space. **A:** Original k-space data. **B:** Image data reconstructed from A, showing good image contrast and spatial resolution. **C:** Center portion of k-space. **D:** Image data reconstructed from C, showing good image contrast but poor spatial resolution. **E:** Peripheral portion of k-space. **F:** Image data reconstructed from E, showing poor image contrast but good spatial resolution (edges).